

Mechanistic Studies of the Catalytic Reduction of CO₂ to CO: Efficient CO-Releasing Si- and Ge-Based Catalysts

Taye B. Demissie* and Jenbrie M. Kessete*

Cite This: *ACS Omega* 2022, 7, 4694–4702

Read Online

ACCESS |



Metrics & More

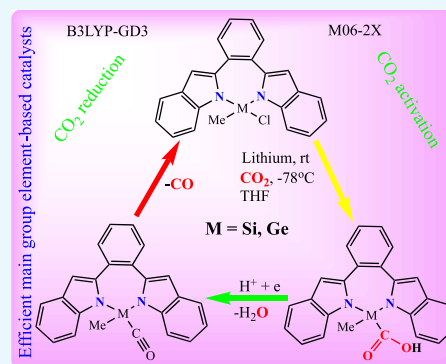


Article Recommendations



Supporting Information

ABSTRACT: Besides its significant challenges, efficient catalytic conversion of CO₂ to value-added chemicals is highly desired. Herein, we report efficient silicon- and germanium-based catalysts for CO₂ activation and its reduction to CO studied using B3LYP-GD3/6-31++G(d,p)/tetrahydrofuran (THF) and M06-2X/6-311++g(d,p)/THF density functional theory methods. The catalysts were systematically designed based on the previously reported silicon- and germanium-based compounds. The germanium-based catalysts are reported for the first time in this study. The calculated transition state energy barriers (5.7–15.8 kcal/mol) indicate that all the catalysts can easily activate CO₂. Among all the B3LYP-GD3-calculated transition-state energy barriers, the highest energy barrier found (27.2–28.3 kcal/mol) is for the protonation of the carboxylic acid group of the silacarboxylic and germacarboxylic acids. Once the silacarboxylic and germacarboxylic acids are protonated, the water molecule can easily dehydrate and leave the catalysts with CO. The electrochemical reduction of the M–CO (M = Si and Ge) complexes further enhances the complexes to easily release CO, with all transition state energy barriers being lower than 10 kcal/mol. The results show that both CO₂ activation and its reduction to CO using the studied catalysts are thermodynamically and kinetically favorable. This work provides an important insight for CO₂ activation and its reduction to CO using earth-abundant and nontoxic main group element-based catalysts.



INTRODUCTION

The over-utilization of natural resources is implacably fueling the emission of carbon dioxide (CO₂) into the atmosphere. According to the World Meteorological Organization, the CO₂ concentration has exceeded the 400 ppm milestone in 2015.¹ The world is joining forces toward research and development aimed at slowing or reducing the amount of CO₂ emission to the atmosphere.² In this regard, the utilization of carbon dioxide as a C1 source for the synthesis of fine chemicals provides an attractive alternative to compounds presently derived from coal and petroleum.³ Besides this, it is an economical and renewable source.⁴ The past decades have witnessed significant progress in the use of carbon dioxide in chemical synthesis owing to the long-standing challenge to chemists to utilize simple and easily accessible feedstock^{2a,5} for the synthesis of structurally complex and high-value molecules.^{2a,6}

The effective transformation of carbon dioxide into useful value-added chemicals will inescapably rely on catalysts.^{3b,c,7} The issue at hand is that carbon dioxide is a very thermodynamically and kinetically stable molecule. However, it has been demonstrated that the molecule can be activated and converted to value-added chemicals using varieties of catalysts.⁸ There are only few cases where the balance between the created value of the product and the cost of the required energy input is economically favorable. Besides other interdependent factors that have an impact on this balance, a

more efficient and controlled activation of CO₂ would allow one to increase the molecular complexity of the product and decrease the level of energy input and as a consequence the added value of the compounds synthesized from CO₂.^{2a,3a–c,6c,d,7,8,9}

Although transition-metal complexes have been used successfully to activate small molecules,^{6a,c,d,7,10} methods which employ systems that move away from transition metals hold special interest. In this context, in recent years, metal-free homogeneous catalysis has emerged as a sustainable approach¹¹ because of milder reaction conditions by which CO₂ can be activated and reduced into various value-added products.¹² Metal-free catalytic systems for the activation and reduction of CO₂ offer the development of chemical processes with low cost, earth-abundant nature, nontoxic nature, and by utilizing low carbon footprints.^{12b,13} This is also because main group-based systems are cheaper and greener alternatives to transition-metal systems.¹⁴

Received: December 18, 2021

Accepted: January 12, 2022

Published: January 27, 2022



In the past few years, there have been many important developments in the design of metal-free catalytic systems for the activation of carbon dioxide.^{12b,13,15} Among these are phosphine-borane-, silylene-, and germanium-based catalysts.^{10c,13,14,16} In this regard, the chemistry of stable acyclic silylenes has evolved considerably over recent decades and gained much attention owing to their ability to selectively activate small molecules. Compared to carbenes, silylenes generally have a singlet ground state as opposed to the ground electronic state of carbenes, which exhibit a singlet or triplet state depending on the nature of the substituents attached to the molecule.^{10c} Besides, silyl groups (R₃Si) are also good protecting groups in organosilicon chemistry. The removal of the silyl groups can be facilitated by reaction with acids or fluorides.^{17,18} Singlet-state silylenes have frontier molecular orbitals with a high-energy lone pair and a vacant p-orbital. This gives them an acceptor/donor character which mimics the frontier d-orbitals that are found in transition metals. This made it possible for acyclic silylenes to activate inert molecules such as CO₂, a process that was known previously to be exclusive to transition metals. Even though there are reports on the use of silyl and silylene complexes for the activation of small molecules, germanium-based catalysts are not well explored in activating CO₂.

Therefore, to provide a focused perspective on the activation of CO₂ using metal-free catalysts, this work presents a computational study on selected silyl and germyl-based metal-free catalyzed reactions toward the activation and reduction of CO₂. Density functional theory (DFT) calculations were employed to investigate the catalysts' ability to activate CO₂ and consequently reduce it to carboxylic acid derivatives and carbon monoxide. To the best of our knowledge, detailed reaction mechanisms for CO₂ activation and its reduction via the formation of silacarboxylic and germacarboxylic acids are reported for the first time in this work.

The structures of eight catalysts, namely, chloro(methyl)diphenylsilane (1), chlorodiphenyl(trifluoromethyl)silane (2), chloro(methyl)diphenylgermane (3), chlorodiphenyl(trifluoromethyl)germane (4), 11-chloro-11-methyl-11H-benzo[5,6][1,3,2]diazasilepino[1,7-*a*:3,4-*a'*]diindole (5), 11-chloro-11-(trifluoromethyl)-11H-benzo[5,6][1,3,2]diazasilepino[1,7-*a*:3,4-*a'*]diindole (6), 11-chloro-11-methyl-11H-benzo[5,6][1,3,2]diazagermepino[1,7-*a*:3,4-*a'*]diindole (7), and 11-chloro-11-(trifluoromethyl)-11H-benzo[5,6][1,3,2]diazagermepino[1,7-*a*:3,4-*a'*]diindole (8), considered for the activation and reduction of CO₂ in this work are presented in Figure 1.

RESULTS AND DISCUSSION

CO₂ Activation. The synthetic procedure of chloro(methyl)diphenylsilane toward (methyl)diphenylsilyl)lithium has been reported by Friis et al.,¹⁹ whereas (diphenyl(trifluoromethyl)silyl)lithium and (diphenyl(trifluoromethyl)germyl)lithium were adopted and reported for the first time in this work. Methyl-diphenylchlorosilanes can also be prepared using an already established procedure.²⁰ On the other hand, the 1,2-bis(indol-2-yl)benzene ligand, which can be easily prepared by a coupling reaction of 2-borylindole with 1,2-diiodobenzene, was reported by Tanaka and Osuka,²¹ where the authors demonstrated that the tetracoordinated silicon complexes of this ligand exhibit blue emission in solution with high efficiency. To the best of our knowledge, the

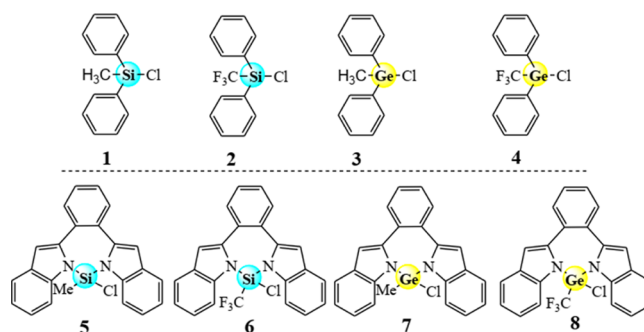
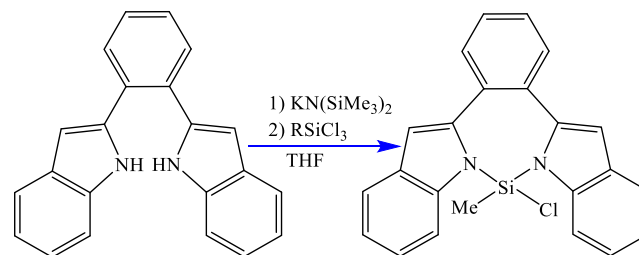


Figure 1. Structures of the eight silicon- and germanium-based catalysts.

tetracoordinated silicon and germanium complexes of this ligand are not used in CO₂ activation and reduction. Unlike the previous study, we here used trichloro(methyl)silane and trichloro(methyl)germane for the proposed synthesis of the catalysts (Scheme 1).

Scheme 1. Synthetic Route for the Tetracoordinated Silicon Complexes Using the 1,2-Bis(indol-2-yl)benzene Ligand



The use of the silicon and germanium complexes of this ligand for either CO₂ capture or reduction is reported for the first time in this work. In the pre-CO₂ capture reaction, lithium is used mainly due to its stronger reducing agent and has a greater tendency to lose electrons.²² We analyzed the heterolytic and homolytic cleavage of the R₃Si–Li bond while capturing CO₂. If heterolytic cleavage is considered, R₃Si becomes an anion together with the lithium cation, whereas the R₃Si radical forms together with the lithium atom when homolytic cleavage is considered. The energy analysis supports the homolytic cleavage and leaves the R₃Si–CO₂ as an open-shell (doublet) molecule. This makes it very reactive. It is to be noted that a related procedure has been used for the synthesis of silacarboxylic acids.¹⁹ The same procedure has been followed for the germanium derivatives. The overview of the reactions considered for CO₂ activation and reduction reactions is depicted in Figure 2.

The aryl groups could cooperate as additional nucleophilic groups with the reactive sites of the silicon center, facilitating its cooperative reactivity. As already known, the lowest unoccupied molecular orbital (LUMO) of the CO₂ molecule is found on the carbon atom, while the highest occupied molecular orbital (HOMO) is found on the oxygen atoms (Figure S1). This is further supported by the spin density, which is populated on the oxygen atoms of CO₂ (Figure 3). This means that the carbon center reacts with nucleophiles and the oxygen centers are susceptible to electrophilic addition reaction. This is evident from the structures that both silicon and germanium atoms of the complexes attach to the carbon

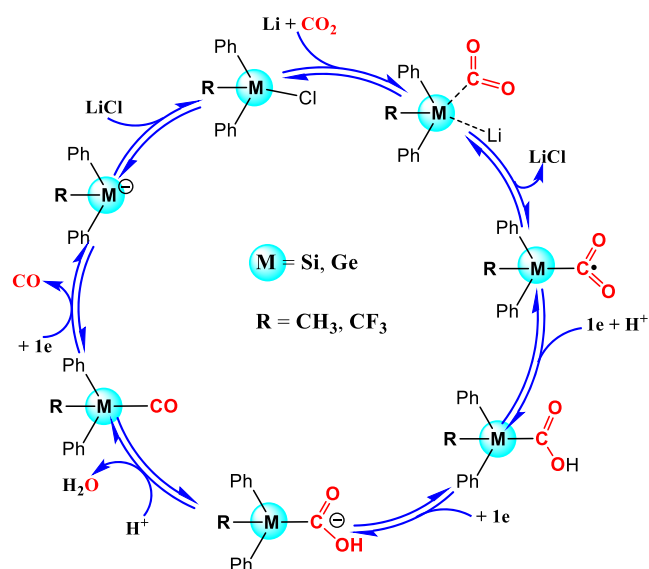


Figure 2. Overview of the mechanistic components and steps for the activation and electrochemical reduction of CO_2 examined in this work; we used HCl as a source of proton according to the literature.¹⁹

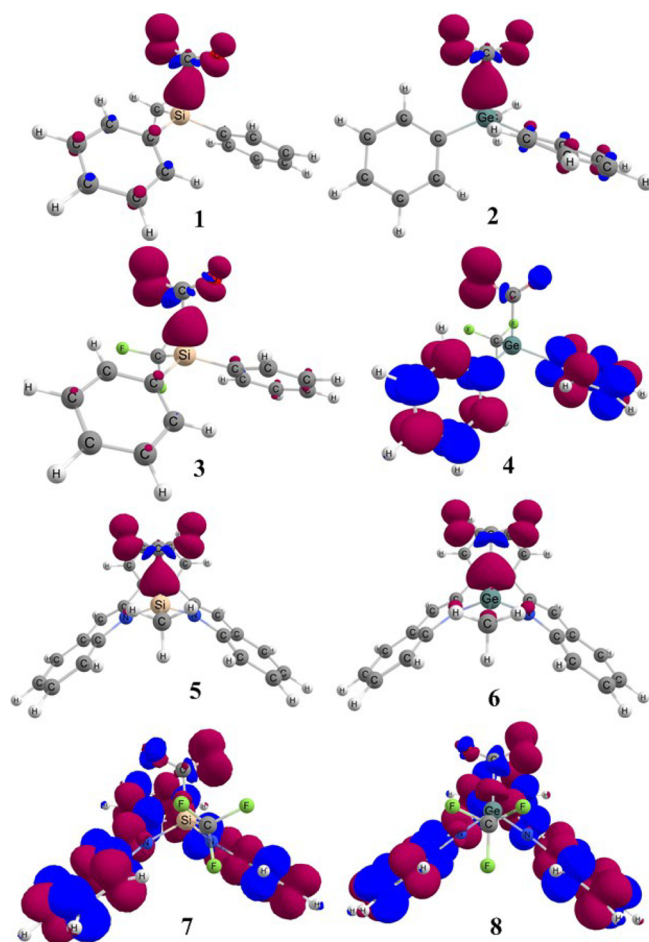


Figure 3. Spin density plots for the eight complexes with activated CO_2 calculated using B3LYP/6-31++G(d,p)/THF. A contour value of 0.008 a.u. was used for all the plots. Dark red represents positive spin density and blue represents negative spin density.

atom of CO_2 . Moreover, the considerable spin density on the oxygen atoms further enhances the protonation process.

The spin density plays an important role on the interaction of CO_2 with the active part of the catalyst. The high spin density is localized on the oxygen atom of CO_2 . For the high spin to become paired, an extra electron of opposite spin is acquired. Complexes 1, 2, 5, and 6 of Figure 3 show a higher spin density on Si- CO_2 and Ge- CO_2 bonds than other complexes, which could be due to the methyl group attached to Si and Ge. On the other hand, there is a similar spin population in complex 3 where there is high spin density localized at the O and Si atoms. This indicates a favorable condition for the formation of strong Si- CO_2 and Ge- CO_2 bonds. Complex 4 also shows a high spin density on phenyl that weakens the Ge- CO_2 bond. The spin density of the Si- CO_2 bond in complex 5 is larger than that of the spin density of Si- CO_2 in complex 7. The spin density of the 1,2-bis(indol-2-yl)benzo group on the complexes increases when CH_3 is replaced with CF_3 . Moreover, the electronic structure of complexes 7 and 8 is illustrated by the spin density, which is localized almost over the whole structure.

Both silicon and germanium complexes activate CO_2 when the silicon and germanium atoms interact with the carbon center since there is an electronic transfer from the electron-rich Si to the electrophilic carbon center. In such coordination with the electron-rich silicon and germanium centers, there is a geometric transformation of the CO_2 from a linear to bent state. This is a result of the rehybridization of the carbon atom following the LUMO of CO_2 getting populated.⁸ The calculated activation energy barriers for CO_2 activation range from 9.9 to 15.7 kcal/mol for catalysts 1–4, the lowest being that of 4 (vide infra)(Figure 4). The transition states and the energy barriers for the CO_2 binding to the catalysts indicate that all the reactions are experimentally accessible reactions. Carbon dioxide activation using catalysts 5–8 showed energy barriers less than 10 kcal/mol, the smallest barrier (5.70 kcal/mol) being for that of 6 (Figure 5).

In agreement with the calculated structures, the predominant component of the HOMO found in the transition state (TS) is attributed by the interaction with the LUMO orbital of the CO_2 molecule (Figure S1). The catalysts stabilize the CO_2 molecule in its bent form in the TS while maintaining the electrophilic nature of the carbon atom and a weak interaction between the lone pairs of one of the oxygen atoms of CO_2 (Figure S1). The mechanism involves electron delocalization across the electrophilic and nucleophilic centers and begins with isolated or separate sites of electron donation and acceptance.¹⁶ In general, all the eight silicon- and germanium-based catalysts are found to easily activate CO_2 .

Silicarboxylic and Germacarboxylic Acids. Silicarboxylic acids have been experimentally found to be efficient carbon monoxide-releasing molecules and used, for instance, in the synthesis of bioactive molecules.¹⁹ In this regard, silicarboxylic and germacarboxylic acids have been previously reported.^{19,23} It has also been indicated that silicarboxylic acids are demonstrated to be easy to handle, air-stable,²³ and efficient carbon monoxide precursors.¹⁹ This has been demonstrated in the synthesis of important bioactive compounds such as HIV-1 inhibitor.¹⁹ Besides these, silylation—introduction of a substituted silyl group (R_3Si) to a molecule—is an important basis of organosilicon chemistry. In this regard, the reaction mechanisms for the syntheses of silicarboxylic and germacarboxylic acids by themselves are worth detailed consideration. Hence, in this work, we studied the reaction mechanisms for the reactions leading to the formation of

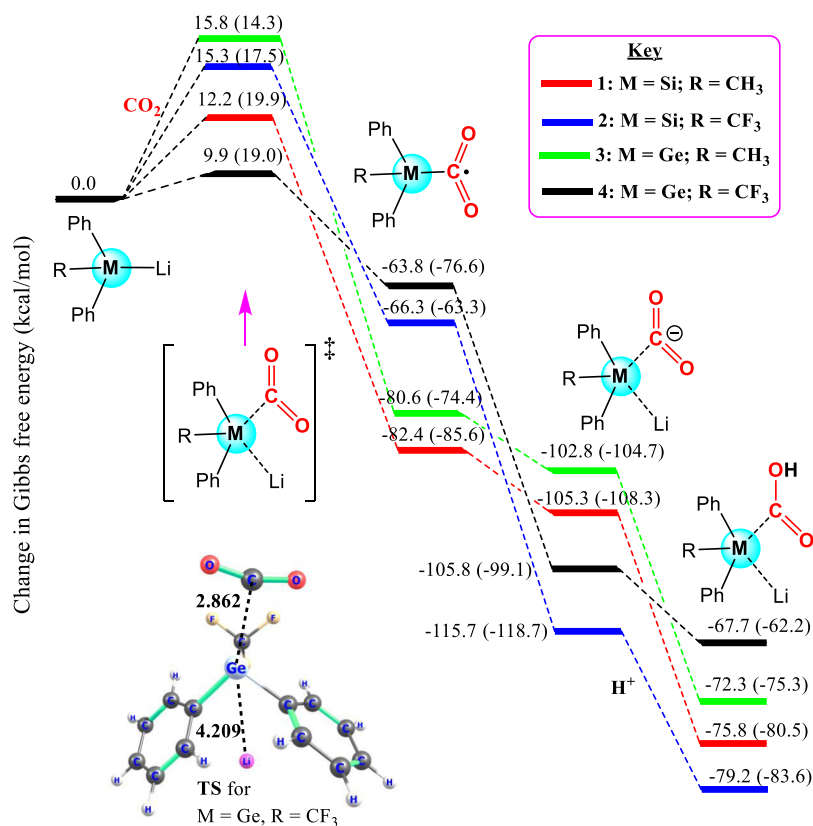


Figure 4. Energy diagram for the activation of CO₂ using catalysts 1–4 and the subsequent reductions leading to the formation of silacarboxylic and germacarboxylic acids. HCl was used as a source of proton. All the changes in energies are reported in kcal/mol. Those without the parenthesis were calculated using B3LYP-GD3/6-31++G(d,p)/PCM(THF), and those in the parenthesis were calculated using M06-2X/6-311++G(d,p)/PCM(THF). The energies are ordered based on the B3LYP-GD3 results.

silacarboxylic and germacarboxylic acids. The experimental reaction for the reaction shown on the left-hand side of Scheme 2 was reported by Friis et al.,¹⁹ whereas the reaction shown at the right-hand side is proposed for the first time in this work. However, it has been suggested that silacarboxylic and germacarboxylic acids can be easily synthesized in high yield from the corresponding silyl- and germyl chlorides through treatment with lithium and reaction with CO₂.^{18,22} In such reactions, HCl was used as a source of proton.^{18,21} The same procedures were considered for the germanium-based catalysts investigated in this work.

The energy diagram for the reaction leading to the formation of the carboxylic acid derivatives is presented in Figures 4 and 5. The intermediate products with activated CO₂ using catalysts 1–4 are exergonic reactions for all the reactions considered (Figure 4). The relative energies from M06-2X functional calculations within parenthesis also show easy CO₂ reduction and exergonic reaction steps (Figure 4). The relative Gibbs free energies in parenthesis are calculated from the electronic energies presented in Table S1. The results range between –63.8 and –82.4 kcal/mol. This indicates that the activated CO₂ bound to both silicon and germanium centers is stabilized. Upon reduction, the intermediate product becomes further stabilized in all the catalysts studied, which can subsequently be changed to the carboxylic acid derivatives upon protonation. Like reactions catalyzed by 1–4, the change in Gibbs free energies for the electrochemical and the protonation reactions catalyzed by 5–8 are also all exergonic (Figure 5). All the calculated changes in Gibbs free energies show that the reactions leading to the formation of the

silacarboxylic and germacarboxylic acids precede easily. This is in agreement with the previously reported experimental results.^{18,22}

Selected structural parameters are listed in Table 1. As expected, the Si–C and Ge–C bond lengths at the transition state are longer than those of the complexes with activated CO₂. Upon reduction of the complexes with activated CO₂, these bond lengths decreased, indicating further stabilization of these CO₂ activated complexes. The same bond lengths after protonation (carboxylic acids) do not show considerable changes.

Path to CO Release. Silicon-containing compounds are very important in organosilicon chemistry, being used as functional materials and building blocks.²⁰ Among them, silacarboxylic and germacarboxylic acids take the prominent position as a source of silyl and germyl radicals which are important intermediates for the synthesis of organosilicon and organogermanium compounds.²² Silacarboxylic acids have also a potential in releasing CO at ambient temperature with a fluoride source.¹⁸ It has also been indicated that the decarboxylation of silacarboxylic and germacarboxylic acids proceeds smoothly in the presence of a photocatalyst and results in the formation of silyl and germyl radicals.²² In the present work, we computationally investigated the ability of four silacarboxylic acids and four germacarboxylic acids in releasing CO. We used electrochemical process as an external stimulation to release CO accompanied by the simultaneous addition of a proton and an electron to the intermediate products. The calculated energy diagram for the path leading to the release of CO from the silacarboxylic and germacarbox-

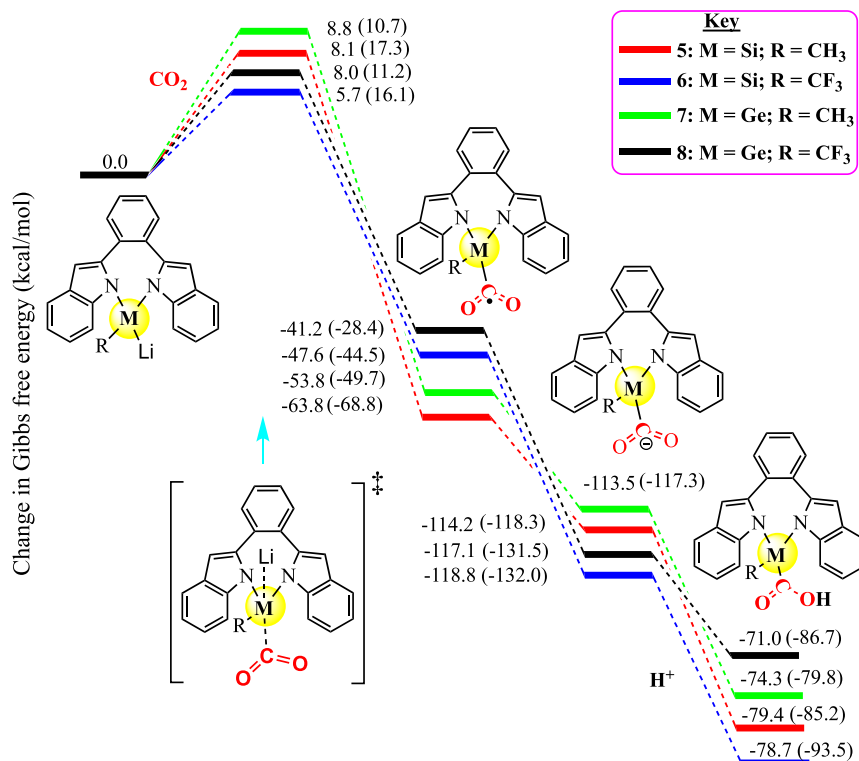


Figure 5. Energy diagram for the activation of CO₂ using catalysts 5–8 and the subsequent reduction, leading to the formation of silacarboxylic and germacarboxylic acids. All the changes in energies are reported in kcal/mol. Those without the parenthesis were calculated using B3LYP-GD3/6-31++G(d,p)/PCM(THF) and those in the parenthesis were calculated using M06-2X/6-311++G(d,p)/PCM(THF).

Scheme 2. Synthetic Procedures of Silacarboxylic Acids from Chlorosilanes

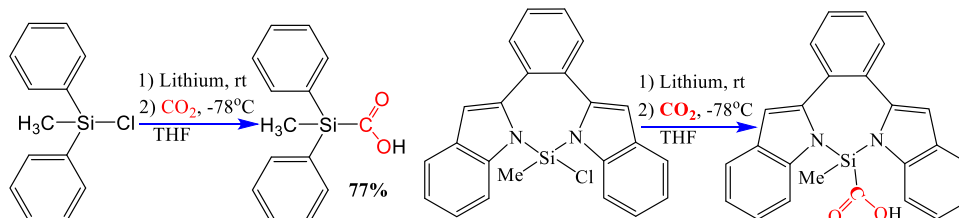


Table 1. Selected Structural Parameters (Å) for the Activation and Reduction of CO₂ Using Catalysts 1–8

catalysts	M–CO ₂ (TS)	M–CO ₂ (activated)	M–CO ₂ (1e reduced)	M–COOH
Methyldiphenylsilyl- and Methyldiphenylgermyl-Based Catalysts				
1: M = Si, R = CH ₃	3.18728	2.16409	1.94607	1.94780
2: M = Si, R = CF ₃	2.93511	2.13489	1.94198	1.93600
3: M = Ge, R = CH ₃	3.12527	2.30453	2.01879	2.00921
4: M = Ge, R = CF ₃	2.86174	2.25921	2.01872	1.99722
1,2-Bis(indol-2-yl)benzoyl- and 1,2-Bis(indol-2-yl)benzogermyl-Based Catalysts				
5: M = Si, R = CH ₃	3.03045	2.11060	1.92852	1.93287
6: M = Si, R = CF ₃	2.72891	1.95615	1.93748	1.92909
7: M = Ge, R = CH ₃	2.71181	2.27276	2.01677	1.99483
8: M = Ge, R = CF ₃	3.10835	2.12521	2.05321	1.99183

ylic acids (1–4) is presented in Figure 6. Selected structural parameters are presented in Table 2.

The activation energies for the electrochemical protonation of the acids of 1–4 (Figure 6) are calculated to be 27.2, 28.2, 28.3, and 27.9 kcal/mol, respectively, indicating that the protonation reaction proceeds without any difficulty. The visualization of the optimized transition-state structures showed that the O–H distances range from 1.25 to 1.28 Å,

with an imaginary frequency ranging from $i1900$ to $i2100$ cm⁻¹. The Si–C and Ge–C bond lengths slightly change upon protonation (Table 2). However, once the reaction passes the transition state, it easily releases the water molecule, with the C–OH₂ distance ranging from 2.7 to 3.8 Å and leaving Si–CO and Ge–CO molecules. The M–COOH₂ bond distances are longer than the M–COOH bond distances, but the M–CO bond distances are shorter than the M–COOH₂ bond

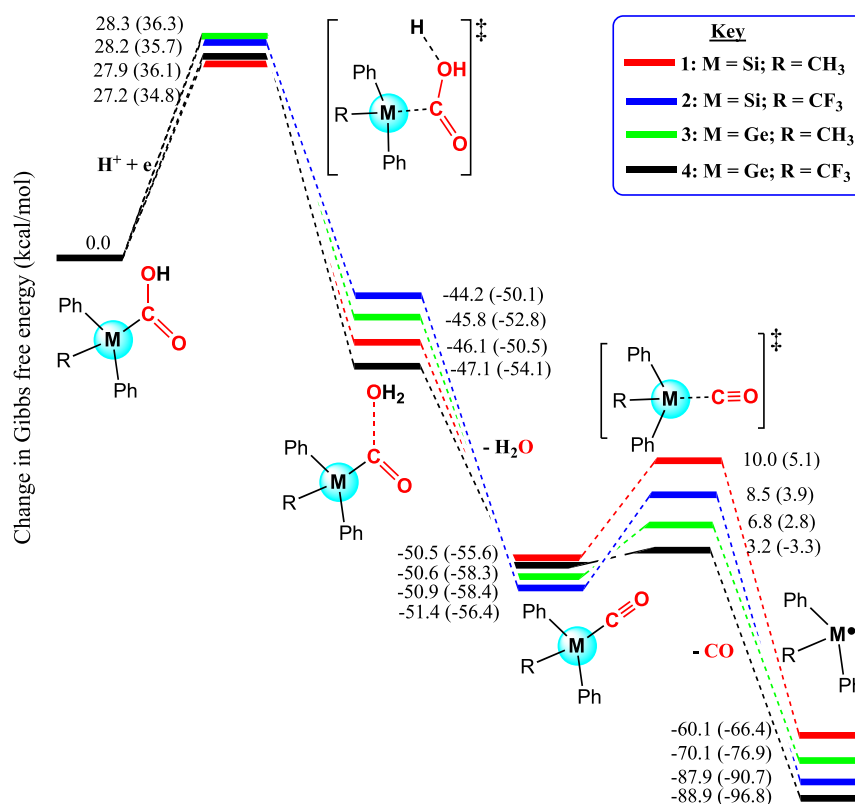


Figure 6. Energy diagram for the reduction of CO₂ via silacarboxylic and germacarboxylic acids of 1–4. All the changes in energies are reported in kcal/mol. Those without parenthesis were calculated using B3LYP-GD3/6-31++G(d,p)/PCM(THF), and those in parenthesis were calculated using M06-2X/6-311++G(d,p)/PCM(THF). The electrocatalytic CO₂ conversion to CO is assumed to use HCl as the proton source.¹⁸

Table 2. Selected Structural Parameters (Å) for Silacarboxylic and Germacarboxylic Acids and Their Reductions Leading toward the Release of CO Using Catalysts 1–8

catalysts	M–COOH	M–COOH ₂ (TS)	M–COOH ₂	MCO–OH ₂	M–CO	M–CO (1e reduced)
Methyldiphenylsilyl- and Methyldiphenylgermyl-Based Catalysts						
1: M = Si, R = CH ₃	1.94780	1.92530	1.97219	3.79405	1.96763	3.83918
2: M = Si, R = CF ₃	1.93600	1.91821	1.94669	2.78254	1.94167	3.71822
3: M = Ge, R = CH ₃	2.00921	2.00709	2.06967	2.92308	2.09082	3.53740
4: M = Ge, R = CF ₃	1.99722	1.97666	2.08653	2.95353	2.07406	3.41574
1,2-Bis(indol-2-yl)benzosilyl- and 1,2-Bis(indol-2-yl)benzogermyl-Based Catalysts						
5: M = Si, R = CH ₃	1.93287	1.90180	1.93272	2.73506	1.94244	3.62041
6: M = Si, R = CF ₃	1.92909	1.86019	1.94048	2.77830	1.93903	4.07710
7: M = Ge, R = CH ₃	1.99483	1.94938	2.06268	2.82339	2.07629	3.76152
8: M = Ge, R = CF ₃	1.99183	2.08068	2.07733	2.72519	2.11424	3.46183

distances and M–CO (1e reduced) bond distances (Table 2). These indicate that further protonation of M–COOH could destabilize the complex and release H₂O to make stable M–CO complexes. Adding a single electron further destabilizes the complexes, and they easily release CO.

All the carboxylic acids based on catalysts 1–8 subsequently release water upon protonation and addition of a single electron to the silacarboxylic acids. The changes in Gibbs free energies (Figures 6 and 7) also show an exergonic reaction for all the investigated carboxylic acids. Since the carbon–silicon and carbon–germanium bonds are highly electron-releasing, they can stabilize the incoming proton on the oxygen atom of CO₂ through hyperconjugation. It is also important to note that a step-by-step reduction and protonation of the carboxylic acids proceed via barrier-less reactions. This indicates a

favorable proton-coupled electron transfer reaction to release H₂O.

As it can be seen from the energy diagram presented in Figure 6 for 1–4, the calculated energy barriers for the release of CO are all less than 10 kcal/mol for 1–4. On the other hand, attempts to get transition-state structures for the CO release reaction from 5 to 8 were not successful since the CO molecule detaches from the catalysts during the geometry-optimization steps. Hence, to further shed light on this final reaction step for 5–8, we performed potential energy surface (PES) scan calculations for the removal of CO from the M–CO complexes of 5–8 (Figure 8). PES scans starting from the M–CO equilibrium bond distance show no barrier. The changes in energies with respect to the M–CO bond distance indicate that the complexes easily release the CO molecule without any energy barrier for 5–8 (Figures 7 and 8). These

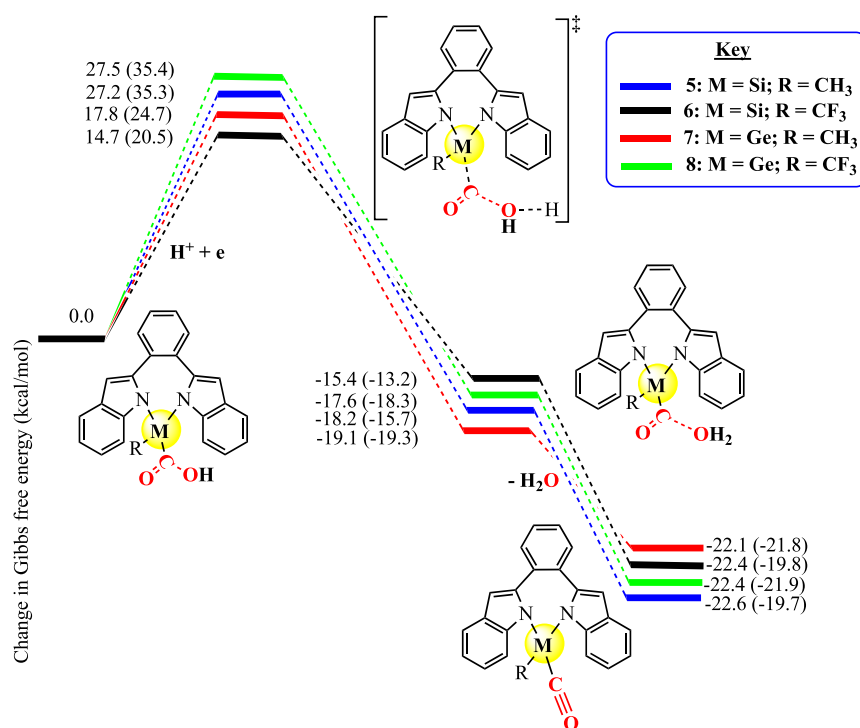


Figure 7. Energy diagram for the reduction of CO₂ path via silicarboxylic and germacarboxylic acids of 5–8. All the changes in energies are reported in kcal/mol. Those without the parenthesis were calculated using B3LYP-GD3/6-311++G(d,p)/PCM(THF), and those in the parenthesis were calculated using M06-2X/6-311++G(d,p)/PCM(THF). The energies are ordered based on the B3LYP-GD3 results.

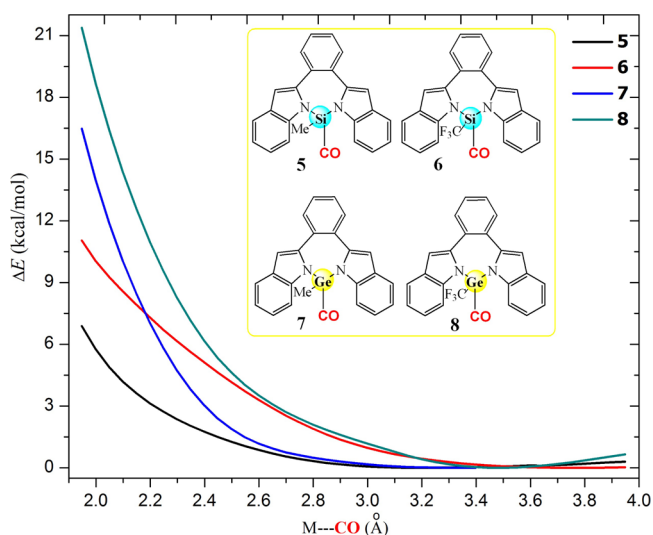


Figure 8. PES scans for the Si–CO and Ge–CO bond distances (in Å) for 5–8 calculated using B3LYP-GD3/6-311++G(d,p)/PCM(THF). The changes in energies were calculated with respect to the energy of the minimum structures on the PES.

reaction steps lead to the formation of silyl and germyl radicals. However, if an electrochemical process is used as a stimulus, the reaction proceeds without any energy barrier. After releasing CO, the catalysts could remain as anions or radicals, which can easily undergo either reaction with the lithium ion to regenerate the catalysts or undergo the silylation reaction in which the silyl group further binds itself to CO₂. Test calculations for the reactions between the catalyst radicals (Figure S2) indicated that the reactions are not feasible, which could be mainly due to steric effects.

CONCLUSIONS

Novel Si- and Ge-based catalysts and their activities on CO₂ activation and reduction to CO have been investigated and reported. The formation of silicarboxylic acids and germacarboxylic acids from chlorosilane, chlorogermane, CO₂, and HCl requires an overall less than 16 kcal/mol activation energy. On the other hand, CO₂ activation with 1, 2-bis(indol-2-yl)benzosilyl (5, 6)- and 1,2-bis(indol-2-yl)benzgermyl (7, 8)-based catalysts has an energy barrier of less than 8.8 kcal/mol. Cleavage of the C–OH bond through the protonation of silicarboxylic acid and germacarboxylic acid has an energy barrier less than 29 kcal/mol, which is higher than the activation energy required to release CO (10 kcal/mol), indicating that it is the rate-determining step. Further protonation of M–COOH destabilizes the complexes and facilitates the easy release of H₂O to make stable M–CO molecules. Single-electron reduction of the M–CO molecules further destabilizes the complexes and facilitates an easy release of CO. Our results demonstrate that the reported silicon- and germanium-based catalysts are efficient in CO₂ activation and its reduction to CO. The study on the catalytic activity of these eight metal-free catalysts also sheds more light on the study and application of main-group element-based catalysts for CO₂ activation and reduction reactions. The calculated results for the silicon-based catalysts agree well with the previously reported experimental results, which used related catalysts as efficient CO-releasing molecules. However, further experimental studies on the germanium-based catalysts are very important to confirm our calculated results.

COMPUTATIONAL DETAILS

All the calculations were carried out using the full structural models of the ligands without symmetry constraints. The

restricted formalism was employed for the closed-shell models and the unrestricted formalism for the open-shell models. The calculations were performed using the Gaussian 16 program package (version G16-C.01).²⁴ The geometries of the molecules involved in the reaction mechanisms were optimized using the B3LYP²⁵ functional together with Grimme's dispersion correction²⁶ (labeled B3LYP-GD3) and the 6-31++g(d,p)²⁷ basis set. Previously calculated results on related reactions indicated that the activation and reaction energies computed at the B3LYP-GD3 level either follow the same trends or are close to the reference SCS-MP2 results.²⁸ It has also previously been demonstrated that the 6-31++G(d,p)²⁹ basis set is appropriate for DFT studies of such reactions. The optimized geometries were confirmed to be the real minima on the PES with no imaginary frequencies by performing a vibrational analysis at the same level of theory. The transition-state calculations were calculated using the quadratic synchronous transit (QST3) method,³⁰ which requires not only an initial guess for the transition-state geometry but also the optimized structures of the reactants and products. The optimized transition-state structures were confirmed by the presence of an appropriate single imaginary vibrational frequency. To mimic the experimental conditions, we used the polarizable continuum model (PCM)³¹ in its integral equation formalism variant (IEF-PCM)³² together with the tetrahydrofuran (THF) solvent. The changes in Gibbs free energies were all calculated at 298.15 K and 1 atm. All the low-frequency modes were also taken into consideration during the analyses of the Gibbs free energies. In addition to B3LYP-GD3, we also used the M06-2X³³ functional together with the 6-311++G(d,p) basis set for single-point energy calculations on the structures optimized using the former functional. It is important to note that the M06-2X functional is well suited for a broad range of applications on main-group chemistry,³³ and we believe that it further refines the energy values. Solvent effects were treated using the same way as the B3LYP-GD3 calculations. The electronic single-point energies computed using M06-2X/6-311++G(d,p) (E_{M2}) were converted to Gibbs free energies (G_{M2}) using the following relation

$$G_{M2} = G_{M1} - E_{M1} + E_{M2}$$

where the M_1 refers to the results calculated using B3LYP-GD3/6-31++G(d,p)/THF and M_2 using M06-2X/6-311++G(d,p)/THF.

The free energy barriers (ΔG^\ddagger) for the TSs of activation of CO₂ were calculated relative to the free catalysts and CO₂. Similar procedures were used for the other energy barrier calculations.

■ ASSOCIATED CONTENT

SI Supporting Information

The Supporting Information is available free of charge at <https://pubs.acs.org/doi/10.1021/acsomega.1c07142>.

Cartesian coordinates of the optimized structural models used in the calculations (PDF)

■ AUTHOR INFORMATION

Corresponding Authors

Taye B. Demissie – Department of Chemistry, University of Botswana, Gaborone 0074, Botswana; orcid.org/0000-0001-8735-4933; Email: sene3095@gmail.com

Jenbrie M. Kessete – Department of Chemistry, Addis Ababa University, Addis Ababa 1176, Ethiopia;
Email: jenbriemolla@gmail.com

Complete contact information is available at:
<https://pubs.acs.org/10.1021/acsomega.1c07142>

Notes

The authors declare no competing financial interest.

■ ACKNOWLEDGMENTS

The authors acknowledge the Departments of Chemistry of Addis Ababa University and the University of Botswana for the research facilities. Computational resources were supplied by the project “e-Infrastruktura CZ” (e-INFRA CZ ID: 90140) supported by the Ministry of Education, Youth and Sports of the Czech Republic.

■ REFERENCES

- (1) (a) Betts, R. A.; Jones, C. D.; Knight, J. R.; Keeling, R. F.; Kennedy, J. J. El Niño and a record CO₂ rise. *Nat. Clim. Change* **2016**, *6*, 806–810. The World Meteorological Organization. *The State of Greenhouse Gases in the Atmosphere Based on Global Observations through 2015*; The World Meteorological Organization, 2016.
- (2) (a) Aresta, M. Carbon Dioxide: Utilization Options to Reduce its Accumulation in the Atmosphere. *Carbon Dioxide as Chemical Feedstock*; John Wiley & Sons, 2010; pp 1–13. (b) Lee, M.-Y.; Park, K. T.; Lee, W.; Lim, H.; Kwon, Y.; Kang, S. Current achievements and the future direction of electrochemical CO₂ reduction: A short review. *Crit. Rev. Environ. Sci. Technol.* **2020**, *50*, 769–815.
- (3) (a) Lee, M.-Y.; Park, K. T.; Lee, W.; Lim, H.; Kwon, Y.; Kang, S. Current achievements and the future direction of electrochemical CO₂ reduction: A short review. *Crit. Rev. Environ. Sci. Technol.* **2020**, *50*, 769–815. (b) Liu, A.; Gao, M.; Ren, X.; Meng, F.; Yang, Y.; Gao, L.; Yang, Q.; Ma, T. Current progress in electrocatalytic carbon dioxide reduction to fuels on heterogeneous catalysts. *J. Mater. Chem. A* **2020**, *8*, 3541–3562. (c) Nitopi, S.; Bertheussen, E.; Scott, S. B.; Liu, X.; Engstfeld, A. K.; Hørch, S.; Seger, B.; Stephens, I. E. L.; Chan, K.; Hahn, C.; Nørskov, J. K.; Jaramillo, T. F.; Chorkendorff, I. Progress and Perspectives of Electrochemical CO₂ Reduction on Copper in Aqueous Electrolyte. *Chem. Rev.* **2019**, *119*, 7610–7672.
- (4) Bontemps, S. Boron-mediated activation of carbon dioxide. *Coord. Chem. Rev.* **2016**, *308*, 117–130.
- (5) van Leeuwen, P. W. N. M.; Freixa, Z. Carbon Monoxide as a Chemical Feedstock: Carbonylation Catalysis. *Activation of Small Molecules*; John Wiley & Sons, 2006; pp 319–356.
- (6) (a) Zevaco, T.; Dinjus, E. Main Group Element- and Transition Metal-Promoted Carboxylation of Organic Substrates (Alkanes, Alkenes, Alkynes, Aromatics, and Others). *Carbon Dioxide as Chemical Feedstock*; John Wiley & Sons, 2010; pp 89–120. (b) Ballivet-Tkatchenko, D.; Dibenedetto, A. Synthesis of Linear and Cyclic Carbonates. *Carbon Dioxide as Chemical Feedstock*; John Wiley & Sons, 2010; pp 169–212. (c) Mascetti, J. Carbon Dioxide Coordination Chemistry and Reactivity of Coordinated CO₂. *Carbon Dioxide as Chemical Feedstock*; John Wiley & Sons, 2010; pp 55–88. (d) Aomchad, V.; Cristòfol, À.; Della Monica, F.; Limburg, B.; D'Elia, V.; Kleij, A. W. Recent progress in the catalytic transformation of carbon dioxide into biosourced organic carbonates. *Green Chem.* **2021**, *23*, 1077–1113.
- (7) Alvarez, A.; Borges, M.; Corral-Pérez, J. J.; Olcina, J. G.; Hu, L.; Cornu, D.; Huang, R.; Stoian, D.; Urakawa, A. CO₂ Activation over Catalytic Surfaces. *ChemPhysChem* **2017**, *18*, 3135–3141.
- (8) Yin, X.; Moss, J. R. Recent developments in the activation of carbon dioxide by metal complexes. *Coord. Chem. Rev.* **1999**, *181*, 27–59.
- (9) Courtemanche, M.-A.; Légaré, M.-A.; Maron, L.; Fontaine, F.-G. Reducing CO₂ to Methanol Using Frustrated Lewis Pairs: On the

Mechanism of Phosphine–Borane-Mediated Hydroboration of CO₂. *J. Am. Chem. Soc.* **2014**, *136*, 10708–10717.

(10) (a) Beaumier, E. P.; Pearce, A. J.; See, X. Y.; Tonks, I. A. Modern applications of low-valent early transition metals in synthesis and catalysis. *Nat. Rev. Chem.* **2019**, *3*, 15–34. (b) Mason, R. Activation of Small Molecules by Transition Metal Ions and their Complexes. *Nature* **1968**, *217*, 543–545. (c) Fujimori, S.; Inoue, S. Small Molecule Activation by Two-Coordinate Acyclic Silylenes. *Eur. J. Inorg. Chem.* **2020**, *2020*, 3131–3142.

(11) Yadav, S.; Saha, S.; Sen, S. S. Compounds with Low-Valent p-Block Elements for Small Molecule Activation and Catalysis. *ChemCatChem* **2016**, *8*, 486–501.

(12) (a) Cornils, B.; Herrmann, W. A. Concepts in homogeneous catalysis: the industrial view. *J. Catal.* **2003**, *216*, 23–31. (b) Power, P. P. Main-group elements as transition metals. *Nature* **2010**, *463*, 171–177. (c) Stephan, D. W. Frustrated Lewis Pairs: From Concept to Catalysis. *Acc. Chem. Res.* **2015**, *48*, 306–316.

(13) Shan, C.; Yao, S.; Driess, M. Where silylene–silicon centres matter in the activation of small molecules. *Chem. Soc. Rev.* **2020**, *49*, 6733–6754.

(14) Kuriakose, N.; Vanka, K. New insights into small molecule activation by acyclic silylenes: a computational investigation. *Dalton Trans.* **2014**, *43*, 2194–2201.

(15) McCahill, J. S. J.; Welch, G. C.; Stephan, D. W. Reactivity of “Frustrated Lewis Pairs”: Three-Component Reactions of Phosphines, a Borane, and Olefins. *Angew. Chem., Int. Ed.* **2007**, *46*, 4968–4971.

(16) Ménard, G.; Gilbert, T. M.; Hatnean, J. A.; Kraft, A.; Krossing, I.; Stephan, D. W. Stoichiometric Reduction of CO₂ to CO by Phosphine/AlX₃-Based Frustrated Lewis Pairs. *Organometallics* **2013**, *32*, 4416–4422.

(17) (a) Ni, C.; Hu, J. The unique fluorine effects in organic reactions: recent facts and insights into fluoroalkylations. *Chem. Soc. Rev.* **2016**, *45*, 5441–5454. (b) Magnus, P. D.; Sarkar, T.; Djuric, S. 48-Organosilicon Compounds in Organic Synthesis. *Comprehensive Organometallic Chemistry*; Wilkinson, G., Stone, F. G. A., Abel, E. W., Eds.; Pergamon: Oxford, 1982; pp 515–659.

(18) Xu, N. X.; Li, B. X.; Wang, C.; Uchiyama, M. Sila- and Germacarboxylic Acids: Precursors for the Corresponding Silyl and Germyl Radicals. *Angew. Chem., Int. Ed. Engl.* **2020**, *59*, 10639–10644.

(19) Friis, S. D.; Taaning, R. H.; Lindhardt, A. T.; Skrydstrup, T. Silacarboxylic Acids as Efficient Carbon Monoxide Releasing Molecules: Synthesis and Application in Palladium-Catalyzed Carbonylation Reactions. *J. Am. Chem. Soc.* **2011**, *133*, 18114–18117.

(20) Seyferth, D. Dimethyldichlorosilane and the Direct Synthesis of Methylchlorosilanes. The Key to the Silicones Industry. *Organometallics* **2001**, *20*, 4978–4992.

(21) Tanaka, T.; Osuka, A. Tetracoordinate silicon complexes of 1,2-bis(indol-2-yl)benzene as blue-emitting dyes in the solid state. *Chem. Commun.* **2015**, *51*, 8123–8125.

(22) Friis, S. D.; Andersen, T. L.; Skrydstrup, T. Palladium-Catalyzed Synthesis of Aromatic Carboxylic Acids with Silacarboxylic Acids. *Org. Lett.* **2013**, *15*, 1378–1381.

(23) (a) Steward, O. W.; Dziedzic, J. E.; Johnson, J. S. Carboxysilanes and -germanes. II. Synthesis and spectral properties of triorganosilane- and triorganogermanecarboxylic acid. *J. Org. Chem.* **1971**, *36*, 3475–3480. (b) Steward, O. W.; Dziedzic, J. E.; Johnson, J. S.; Frohlinger, J. O. Carboxysilanes and -germanes. III. Ionization constants of triorganosilane- and triorganogermanecarboxylic acids in ethanol-water and dimethyl sulfoxide media. *J. Org. Chem.* **1971**, *36*, 3480–3484.

(24) Frisch, M. J.; Trucks, G. W.; Schlegel, H. B.; Scuseria, G. E.; Robb, M. A.; Cheeseman, J. R.; Montgomery, J. A., Jr.; Vreven, T.; Kudin, K. N.; Burant, J. C.; Millam, J. M.; Lyengar, S. S.; Tomasi, J.; Barone, V.; Mennucci, B.; Cossi, M.; Scalmani, G.; Rega, N.; Petersson, G. A.; Nakatsuji, H.; Hada, M.; Ehara, M.; Toyota, K.; Fukuda, R.; Hasegawa, J.; Ishida, M.; Nakajima, T.; Honda, Y.; Kitao, O.; Nakai, H.; Klene, M.; Li, X.; Knox, J. E.; Hratchian, H. P.; Cross, J. B.; Bakken, V.; Adamo, C.; Jaramillo, J.; Gomperts, R.; Stratmann, R. E.; Yazyev, O.; Austin, A. J.; Cammi, R.; Pomelli, C.; Ochterski, J. W.;

Ayala, P. Y.; Morokuma, K.; Voth, G. A.; Salvador, P.; Dannenberg, J. J.; Zakrzewski, V. G.; Dapprich, S.; Daniels, A. D.; Strain, M. C.; Farkas, O.; Malick, D. K.; Rabuck, A. D.; Raghavachari, K.; Foresman, J. B.; Ortiz, J. V.; Cui, Q.; Baboul, A. G.; Clifford, S.; Cioslowski, J.; Stefanov, B. B.; Liu, G.; Liashenko, A.; Piskorz, P.; Komaromi, I.; Martin, R. L.; Fox, D. J.; Keith, T.; Al-Laham, M. A.; Peng, C. Y.; Nanayakkara, A.; Challacombe, M.; Gill, P. M. W.; Johnson, B.; Chen, W.; Wong, M. W.; Gonzalez, C.; Pople, J. A. *Gaussian 16*, Revision C.01; Gaussian, Inc.: Wallingford CT, 2016.

(25) (a) Becke, A. D. Density-functional thermochemistry. III. The role of exact exchange. *J. Chem. Phys.* **1993**, *98*, 5648–5652. (b) Lee, C.; Yang, W.; Parr, R. G. Development of the Colle-Salvetti correlation-energy formula into a functional of the electron density. *Phys. Rev. B: Condens. Matter Mater. Phys.* **1988**, *37*, 785–789. (c) Stephens, P. J.; Devlin, F. J.; Chabalowski, C. F.; Frisch, M. J. Ab Initio Calculation of Vibrational Absorption and Circular Dichroism Spectra Using Density Functional Force Fields. *J. Phys. Chem.* **1994**, *98*, 11623–11627.

(26) (a) Grimme, S. Calculation of the electronic spectra of large molecules. *Rev. Comput. Chem.* **2004**, *20*, 153–218. (b) Grimme, S.; Furche, F.; Ahlrichs, R. An improved method for density functional calculations of the frequency-dependent optical rotation. *Chem. Phys. Lett.* **2002**, *361*, 321–328.

(27) Krishnan, R.; Binkley, J. S.; Seeger, R.; Pople, J. A. Self-consistent molecular orbital methods. XX. A basis set for correlated wave functions. *J. Chem. Phys.* **1980**, *72*, 650–654.

(28) (a) Douglas-Gallardo, O. A.; Shepherd, I.; Bennie, S. J.; Ranaghan, K. E.; Mulholland, A. J.; Vöhringer-Martinez, E. Electronic structure benchmark calculations of CO₂ fixing elementary chemical steps in RuBisCO using the projector-based embedding approach. *J. Comput. Chem.* **2020**, *41*, 2151–2157. (b) Quattrocchi, D. G. S.; de Oliveira, A. R.; Carneiro, J. W. d. M.; Rocha, C. M. R.; Varandas, A. J. C. MP2 versus density functional theory calculations in CO₂-sequestration reactions with anions: Basis set extrapolation and solvent effects. *Int. J. Quantum Chem.* **2021**, *121*, No. e26583.

(29) (a) García-López, D.; Pavlovic, L.; Hopmann, K. H. To Bind or Not to Bind: Mechanistic Insights into C–CO₂ Bond Formation with Late Transition Metals. *Organometallics* **2020**, *39*, 1339–1347. (b) Simeon, T. M.; Ratner, M. A.; Schatz, G. C. Nature of Noncovalent Interactions in Catenane Supramolecular Complexes: Calibrating the MM3 Force Field with ab Initio, DFT, and SAPT Methods. *J. Phys. Chem. A* **2013**, *117*, 7918–7927.

(30) Xu, X.; Alecu, I. M.; Truhlar, D. G. How Well Can Modern Density Functionals Predict Internuclear Distances at Transition States? *J. Chem. Theory Comput.* **2011**, *7*, 1667–1676.

(31) Tomasi, J.; Mennucci, B.; Cammi, R. Quantum Mechanical Continuum Solvation Models. *Chem. Rev.* **2005**, *105*, 2999–3094.

(32) (a) Cancès, E.; Mennucci, B.; Tomasi, J. A new integral equation formalism for the polarizable continuum model: Theoretical background and applications to isotropic and anisotropic dielectrics. *J. Chem. Phys.* **1997**, *107*, 3032. (b) Mennucci, B.; Tomasi, J. Continuum solvation models: A new approach to the problem of solute's charge distribution and cavity boundaries. *J. Chem. Phys.* **1997**, *106*, 5151.

(33) Wang, Y.; Verma, P.; Jin, X.; Truhlar, D. G.; He, X. Revised M06 density functional for main-group and transition-metal chemistry. *Proc. Natl. Acad. Sci. USA* **2018**, *115*, 10257–10262.